

COVER PAGE

Document downloaded by @DAEL

Sat Nov 28 02:02:43 2026
For personal use

When automatic English translation is provided, only the original document is authentic.
The EAA cannot be held responsible of any translation error

Bibliographical reference

Sound Source Separation on ICE 3 High Speed Trains Based on Combined Sound Pressure and Sound Velocity Measurements, Jean Marc Wunderli, Acta Acustica **vol. 95** (Number 2), 2009, pp. 270-278

DOI
https://doi.org/10.3813/AAA.918149

ACTA ACUSTICA UNITED WITH ACUSTICA
Vol. 95 (2009) 270 – 278
DOI 10.3813/AAA.918149

Sound Source Separation on ICE 3 High Speed Trains Based on Combined Sound Pressure and Sound Velocity Measurements

Jean Marc Wunderli
Empa, Swiss federal laboratories for material testing and research, 8600 Duebendorf, Switzerland

Summary
A measurement method is presented that allows a separation of sound sources based on pass-by measurements of trains. It combines a sound pressure microphone with two sound velocity transducers, all of which are positioned at one point. The velocity transducers are employed as directional microphones. The true source positions and their sound power are determined by solving an inverse problem: In a system of propagation equations the source positions are optimized until a best fit to the measured signals is achieved.
Measurement results are shown for pass-by measurements of German ICE 3 high speed trains at speeds between 200 and 250 km/h. The extended pantographs are thereby identified as dominating sound sources in the upper part of the vehicles. The measurements yield reproducible results and are in accordance with data taken from literature.
The method represents an alternative to the array measurement technique although with a considerably smaller measurement and data analysis effort. Information on the sound power of multiple sources is gathered with an accuracy comparable to array measurements. The localization of the sources is though less precise and the separation is limited to two sources at a time. Therefore the measurement concept can not be seen as a general replacement of the array measurement technique. Nevertheless there is a broad range of applications where a fine spacial resolution is not of major interest. In these cases the method is likely to represent an appropriate substitute.

PACS no. 43.20.Ye

1. Introduction

Tracked vehicles give rise to various sound sources with differing characteristics, depending on the particular vehicle and its operation condition. Over a broad range of velocities rolling noise is the dominating sound source. At low travelling speeds additionally traction noise and cooling noise can become relevant. With increasing speed the importance of aerodynamic sound sources rises. The location of these aerodynamic sources and their sound power relative to rolling noise depend on the type of train and its travelling velocity. According to Dittrich aerodynamic sound can become relevant above 200 km/h and starts to dominate the overall sound emission for speeds greater than 250 km/h [1]. Talotte assumes a slightly higher transition speed around 300 km/h for high-speed trains as the German ICE or the French TGV [2]. Measurements of ICE 3 performed by Martens et al. showed aerodynamic sound equal or superior to rolling noise for travelling velocities of 260 km/h and more [3].

Received 11 July 2008,
accepted 2 January 2009.

A good survey about the locations of these aerodynamic sources can be found in [2]. Prominent sound sources are often detected at the bogies, in the roof section mainly close to the pantographs, at the nose and the rear of the power cars, at inter-coach spacings and other cavities along the vehicle surface.

With regard to sound propagation calculation at least those sources that radiate from heights significantly higher than rolling noise have to be treated separately. As a consequence of their sound propagation paths higher above ground they exhibit less ground effect and shielding effect as well as a lower sensitivity for meteorological effects than the rolling noise sources close to the ground. Accordingly these sound sources at higher positions can yield a relevant contribution to exposure levels even with considerably lower sound power levels than the sources in the lower part of the vehicles.

Noise problems have become a major issue and efforts are made to reduce sound radiation at the source. Sophisticated measurement data that yield separated description of all relevant partial sources are a necessary precondition for that purpose. Such measurement results are also needed as input data for sound propagation models of the newest generation. The railway noise model that was de-

© S. Hirzel Verlag · EAA

veloped within the Harmonoise project [4, 5] distinguishes sound sources at five different heights along the vehicle surface. The calculation model sonRAIL that is actually under way in Switzerland will be based on a comparable source description [6, 7, 8]. Such models can only be applied successfully when according information on the sound radiation of the operating vehicles is at hand. It can be concluded therefore that the demand for measurement technologies that allow for a detailed description of sound sources is likely to increase in the coming years.

A measurement method that proofed its ability to detect secondary sources even when the overall sound exposure is dominated by rolling noise is the array measurement technique. Microphone arrays have been successfully applied to railway noise in several different variations [9, 10, 11, 12, 13]. As a consequence of the great number of microphones involved and the elaborate data analysis the conduction of array measurements is though generally rather laborious and expensive. Therefore efforts have been undertaken to develop an alternative approach for the detection of spatially separated contributions of complex sound sources. The basic idea of the measurement method is to combine sound pressure microphones with sensors featuring a pronounced directivity. As an application of an inverse problem an optimization algorithm is applied that yields for a given number of sources the positions and sound power with which the measured signals can be reproduced best.

The measurement concept has firstly been presented in [14] where signals of a one-dimensional sound-intensity probe were used to identify sound sources other than rolling noise on a freight train. Sound velocity proved to be an appropriate measurement quantity because of the frequency-independent directivity pattern in dependence of the cosine of the angle of incidence. The method was further developed and refined in the frame of a dissertation [15]. It was shown that the possibilities of the method could be improved significantly by adding a second velocity sensor. The resulting measurement concept as well as the data analysis will be explained in section 2. In section 3 measurement results of German ICE 3 high speed trains at travelling speeds between 200 and 250 km/h are presented. Apart from rolling noise the dominating sound sources in the roof section are identified and sound power levels as well as spectra are derived.

2. Measurement and analysis method

2.1. General concept

The measurement technique is based on the combination of a sound pressure microphone and two sound velocity transducers, all of which are positioned at one point. The velocity transducers are employed as directional microphones, as they measure the projection of the sound velocity vector onto the orientation of the sensor. Due to their directional characteristics they allow a focusing towards the regions of most prominent sources, i.e. the wheel and the roof section. One velocity sensor has to be oriented in a way to exhibit a minimal sensitivity towards the wheel and a high sensitivity towards the roof section and the other sensor has to be oriented vice versa.

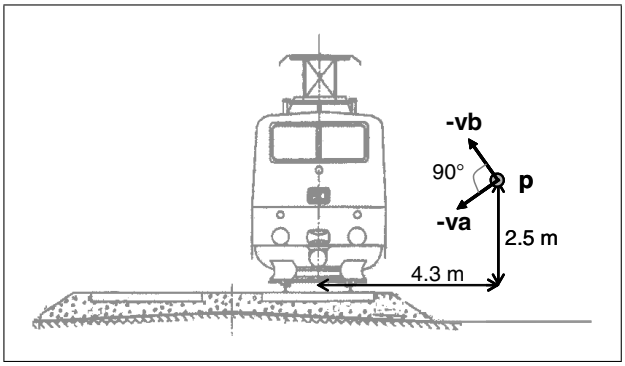


Figure 1. Cross-sectional view of the measurement geometry. p denotes the pressure microphone and v_a respectively v_b are the two velocity sensors.

From numerical simulations a default measurement geometry with a horizontal distance from the middle of the track of 3.75 m and height above track of 3.00 m was derived with an opening angle between the two velocity sensor set to 115°. The position and orientation of the sensors can be varied though, for example to comply with security regulations as it was the case for the measuring campaign presented in this publication, where the distance had to be extended to 4.30 m. Figure 1 shows the geometry that has been used for these measurements. The velocity transducers were oriented with angles of 35.0° respectively -55.0° relative to the horizontal plane.

From the three measurement signals six independent acoustical quantities may be obtained, namely the sound pressure level, two sound intensity level, two sound velocity level and as an additional quantity a cross-velocity level. While the two velocity levels result from squaring the sound velocity signals the latter is calculated by multiplying them. In contrast to the squared velocity signals, that exhibit a directional sensitivity proportional to Cosine squared of the angle of incidence, the cross-velocity has a figure of eight polar pattern with the highest sensitivity in between the orientation of the two velocity sensors. It is intended to enable a measurement focussed on the middle section of the train. Based on the level differences between these quantities the centre of sound radiation may be derived and in a temporal diagram the sound sources can be localized at various heights along the vehicle surface (see Figure 5 as example).

In the data analysis the signals are integrated over a selected time segment of the pass-by and are then applied to a system of propagation equations which simulate the pass-by numerically. The propagation calculation is performed in one-third octave bands and takes into account geometrical spreading, dissipation and ground effect. Dissipation is calculated according to ISO 9613-1 [16]. A simplified model is used to account for the ground reflection that sums up direct sound and reflected sound energeti-

cally. This approach has been chosen as for sources with a strong directivity pattern the geometrically derived reflection point does not represent well the area contributing to the reflection. Therefore phase-sensitive models tend to yield pronounced ground effects that are not seen in measurements.

Equations (1) to (3) show the propagation equations for sound pressure squared, sound intensity and sound velocity squared. The first part of the sum in the integral represents direct sound and the second part the ground reflection.

$$\int_{T1}^{T2} p^2(t)\,\mathrm{d}t = \sum_{n=1}^{N} \frac{W_n \cdot \rho c}{2\pi} \cdot \int_{T1}^{T2} 10^{-0.1\alpha \cdot r_{Dn}(t)} \cdot \frac{\Delta(\psi_{Dn}(t))}{r_{Dn}^2(t)} + 10^{-0.1\alpha \cdot r_{Rn}(t)} \cdot \frac{\Gamma \cdot \Delta(\psi_{Rn}(t))}{r_{Rn}^2(t)}\,\mathrm{d}t \tag{1}$$

$$\int_{T1}^{T2} p(t)\,v(t)\,\mathrm{d}t = \sum_{n=1}^{N} \frac{W_n}{2\pi} \int_{T1}^{T2} 10^{-0.1\alpha \cdot r_{Dn}(t)} \cdot \frac{\cos(\theta_{Dn}(t))\Delta(\psi_{Dn}(t))}{r_{Dn}^2(t)} + 10^{-0.1\alpha \cdot r_{Rn}(t)} \cdot \frac{\Gamma \cdot \cos(\theta_{Rn}(t))\Delta(\psi_{Rn}(t))}{r_{Rn}^2(t)}\,\mathrm{d}t \tag{2}$$

$$\int_{T1}^{T2} v^2(t)\,\mathrm{d}t = \sum_{n=1}^{N} \frac{W_n}{2\pi \cdot \rho c} \cdot \int_{T1}^{T2} 10^{-0.1\alpha \cdot r_{Dn}(t)} \cdot \frac{\cos^2(\theta_{Dn}(t))\Delta(\psi_{Dn}(t))}{r_{Dn}^2(t)} + 10^{-0.1\alpha \cdot r_{Rn}(t)} \cdot \frac{\Gamma \cdot \cos^2(\theta_{Rn}(t))\Delta(\psi_{Rn}(t))}{r_{Rn}^2(t)}\,\mathrm{d}t \tag{3}$$

ρc thereby is the impedance of air, W_n is the sound power of source n, r_{Dn} and θ_{Dn} are the distance and the angle of incidence between source n and the receiver position, α is the atmospheric attenuation coefficient per metre, r_{Rn} and θ_{Rn} are the distance and the angle of incidence for the sound path reflected on the ground and Γ is the energy reflection coefficient. With Δ a directivity of the source can be taken into account in dependence of the radiation angles for direct and reflected sound ψ_{Dn} and ψ_{Rn}.

For a given number and positions of the sources on the vehicle surface the system of equations yields the sound power of each source. As up to six propagation equations can be incorporated the number of equations is generally greater than the number of sources. To solve this overdetermined system of equations the method of 'Singular Value Decomposition' is applied. As the position of the sources is generally not known in advance, an optimization strategy is used that aims at finding the source combination that best reproduces the measured A-weighted level of all included quantities. The system of equations is for this purpose solved for all possible combinations of source positions with source positions provided in equidistant steps along the cross-section of the vehicle surface. Using the resulting sound powers the integration of the pass-by signals is calculated again and compared with the measured values. If the assumed source positions do not agree with the true positions a precise matching can not be achieved. Consequently the source positions that yield best accordance with the measured values are taken as result.

The data analysis is based on the assumption that all sound sources can be reproduced by one or several incoherent point sources. This concept is valid in most cases, but it leads to errors in the case of coherently radiating line sources like vibrating rails. As a consequence the contribution of the rail to the overall rolling noise is underestimated. As shown by Kitagawa and Thompson this restraint also applies to array measurements [17].

The performance of the measurement method and the accuracy of the achievable results depends on several factors:

- The measurement uncertainties.
- The uncertainties of the propagation calculation.
- The number of sources to be separated. The more sources that are incorporated in the system of equations the higher is the sensitivity of the optimization algorithm to the above mentioned uncertainties.
- The position of the sources. The more the considered quantities react to a change of position the better the localisation can be carried out. As the sensitivity of the velocity sensors features the most pronounced angular dependency around angles of incidence of 90°, best results are achieved for source positions in these directions.
- The difference in sound power of the involved sources. As the sources with lower sound power are more affected by uncertainties they can only be identified with a lower accuracy.

The uncertainties of the measurement procedure and the data analysis are discussed in section 2.3 where also a quantification of the accuracy of the measurement results is given. As the measurement uncertainty depends on the sensors used they are presented in following section.

2.2. Instrumentation

There are currently two types of sound velocity sensor available that allow measurements of high accuracy:

- A measurement principle that is known for several decades and is successfully applied for sound intensity and sound power measurements deduces sound velocity from the sound pressure gradient between two microphones (see for example [18]). As for this application sound velocity has to be measured in two directions two pairs of pressure microphones have to be combined. Figure 2 shows a realisation with a spacer specially manufactured to comply with the standard measurement setup described in the previous section. In this

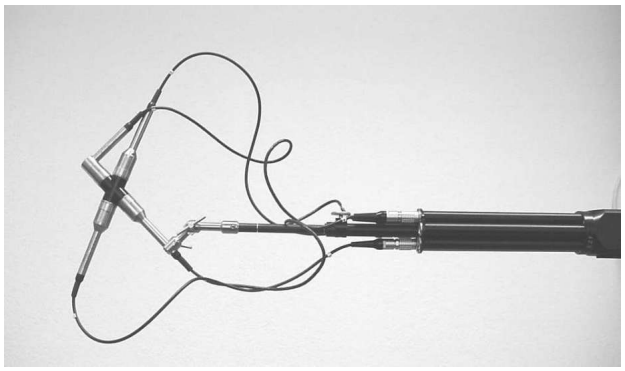


Figure 2. Two-dimensional sound intensity probe with spacings of 22.2 and 22.5 mm. The two probes are separated by an angle of 115°. The two microphone pairs are a GRAS type 50 AI and a Brüel & Kjær type 4177. The handle with the wiring is a GRAS vector intensity probe 50 VI.

configuration a frequency range from 50 Hz to 3.25 kHz can be covered.

- Only available for a few years are probes of the type Microflown. They represent a further development of mass flow sensors and consist of two heated wires. Sound velocity is directly deduced from the temperature difference between the wires, measured by the resistance. As can be seen in Figure 3 the sensors can be highly minimized which allows to combine three velocity sensors and a sound pressure microphone in a single probe. For further details see [19]. The frequency range of the Microflown sensors is generally broader compared to intensity probes. The sensor sensitivity though exhibits a frequency dependency that has to be compensated resulting in a loss of available dynamics.

2.3. Uncertainty

Table I shows the results of the analysis of the measurement uncertainty as performed in [15]. At angles of incidence of high sensitivity the resulting measurement uncertainty is mainly affected by calibration. Especially for the Microflown sensors the secondary calibration, where the sound velocity is referenced to a previously calibrated sound pressure signal, is afflicted by major uncertainties. In the range of low sensor sensitivity the deviations between theoretical and measured directivity dominate the overall uncertainty. Here the Microflown sensors exhibit a higher accuracy. Part of the measurement uncertainty is also the precision with which the sensors can be placed and oriented in the field. While the position can for both sensor types be determined with the same accuracy the angular orientation can be achieved with higher precision for the Microflown sensors. In the analysis of the measurement uncertainty a maximal deviation of the positioning of 2 cm in all directions and a maximal angular error of 1.5° resp. 0.8° was derived for the two sensor types. Regarding the effects of these measurement uncertainties on the resulting uncertainty of the source identification both sensor types are comparable with slight advantages for the intensity probes.

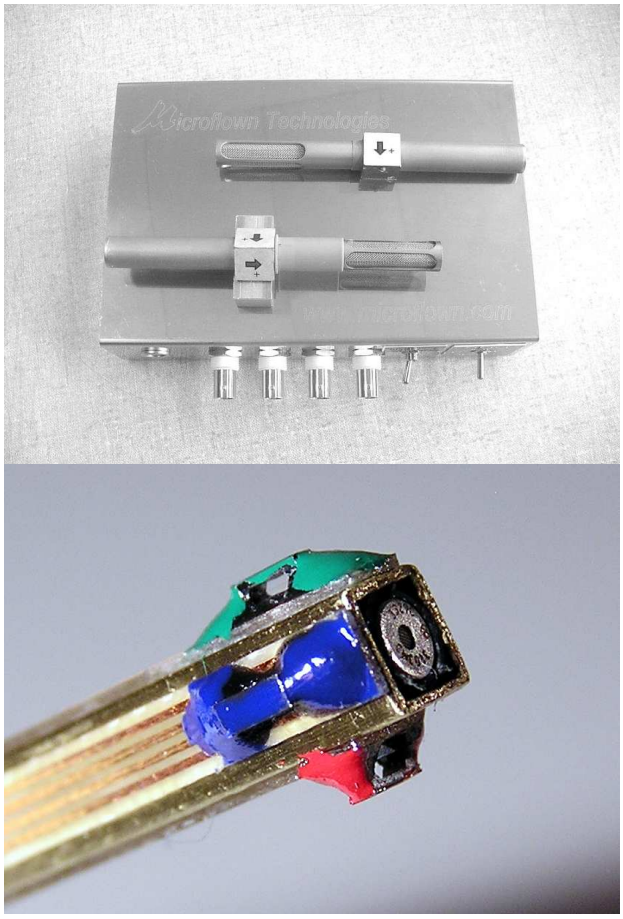


Figure 3. On top two Microflown-probes are depicted. The picture below shows an enlarged view of a three-dimensional Microflown-probe after the protective cap has been removed (photograph courtesy of Microflown). A 0.1 inch sound pressure microphone is visible together with three sound velocity sensors in cartesian orientation.

The uncertainty in the propagation calculation is dominated by the uncertainty stemming from the ground reflection. Based on experiments with loudspeakers placed on the track it could be shown, that with the chosen approach the ground reflection could be reproduced with a standard deviation of approximately 0.5 dB(A). The influence on the uncertainty of the cumulative signal of direct and reflected sound results according to their weights. As a consequence of the measurement geometry the ground reflection can be neglected to a large extent for source position higher above ground.

Based on the above uncertainties numerical simulations according to the Monte-Carlo-method were performed in order to study how the uncertainties affect the accuracy of the resulting source positions and sound powers. It could be shown that best results are gathered when only five propagation equations are used in the system of equations and sound pressure squared is forgone. This finding can be explained as follows: Within the optimization algorithm deviations as a consequence of measurement uncertainties are compensated by shifting the source positions. For quantities featuring a strong directional sensitiv-

Table I. Standard deviations of the measurement uncertainty in dB(A) separated for two types of measurement sensors. As the uncertainty of the sensor directivity pattern, i.e. the deviation between theoretical and measured directivity, shows an angular dependency, values for two angular ranges are given. *h* stands for the range with high sensitivity and is defined as angles of incidence of ± 85°. *l* stands for low sensitivity and covers angles around the local minima. The last line gives the resulting measurement uncertainties calculated according to the rules of error propagation.

	Intensity probe					**Microflown**				
	L_p	L_I(h)	L_I(l)	L_v(h)	L_v(l)	L_p	L_I(h)	L_I(l)	L_v(h)	L_v(l)
primary calibration	0.2	0.2	0.2	0.2	0.2	0.2	0.2	0.2	0.2	0.2
secondary calibration	0.0	0.2	0.2	0.2	0.2	0.4	0.4	0.4	0.4	0.4
atmospheric conditions	0.1	0.1	0.1	0.1	0.1	0.1	0.1	0.1	0.1	0.1
sensor directivity	0.2	0.2	0.7	0.2	1.4	0.1	0.2	0.5	0.2	1.0
	0.3	**0.4**	**0.8**	**0.4**	**1.5**	**0.5**	**0.5**	**0.7**	**0.5**	**1.1**

ity already a small change in position allows to adjust even for prominent errors. In contrast errors in the sound pressure signal can only be compensated through geometrical spreading which causes stronger deviations in the resulting source positions and consequently also in the resulting sound power ratings.

Considering the measurement uncertainties, simulations show that the over-determined system of equations can be solved successfully for situations having up to 15 dB(A) difference between two partial sources. The source strength of the stronger primary source can be derived with a standard deviation of 0.4 dB(A) and the secondary source with a standard deviation of 1.6 dB(A). The source positions can be identified with standard deviations of 0.2 m respectively 0.9 m. The method is not recommended for separating three or more sources as the uncertainty increases notably. Nevertheless test calculations show that even in complex situations the total sound power as well as the centre of radiation can be modelled correctly by assuming only two sources.

An additional, not yet discussed source of uncertainty lies in the assumed directivity pattern of the source. As could be shown in [15] wrong assumptions on the directionality of sound radiation do not lead to a misplacement of the source positions. Errors in sound power are caused though, but only for the concerned source.

3. Measurements of ICE 3 high speed trains

3.1. Measurement setup

Measurements were performed in April 2006 close to a village called Krunkel on the ICE 3-line Köln-Rhein/Main at kilometre 59.2. Figure 4 shows the measurement site during the pass-by of a train. Both types of sound velocity probes were used. As the sound intensity probe available at that moment was just one-dimensional a full data analysis was only possible for the measurements with the Microflown probe. Therefore the results shown in section 3.2 and 3.3 were derived from these signals. It could be proven though in this as well as in other measurement campaigns that both types of velocity senors are suited for this range of application. As additional measurement sensors a three-dimensional ultra-sonic anemometer, also visible in Figure 4, and a light barrier to detect vehicle axes were applied.



Figure 4. Measurement site on the ICE 3-line Köln-Rhein/Main. The black and white arrow indicate the position of the three-dimensional Microflown probe and the GRAS sound intensity probe. Placed in between is a three-dimensional ultra-sonic anemometer to gather information on train-induced turbulence.

3.2. Measurement results

On the nearer track nine pass-bys were measured with train speeds of 196 to 248 km/h. One event with a speed of 240 km/h was sorted out during data analysis because the ultra-sonic-anemometer indicated air movements of more than 10 m/s for a short period. From the remaining eight pass-bys seven were ICE 3 type 403 and one was a ICE 3 type 406. (The latter features a double set of pantographs allowing also for circulation on French railway lines.) Three events F7, F9 and F10 consisted of a single composition with a total length of 200.87 m; the other events were double compositions.

Figure 5 shows a temporal diagram of a pass-bys for the sound pressure level and the two sound velocity levels that result from squaring the velocity signals. Additionally displayed are the level differences between the sound pressure level and the two sound velocity levels. These differences give hints on the centre of gravity of sound radiation. Because of the dominating rolling noise the level difference between sound pressure and the velocity of sensor *a* reaches a minimum at each time a bogie

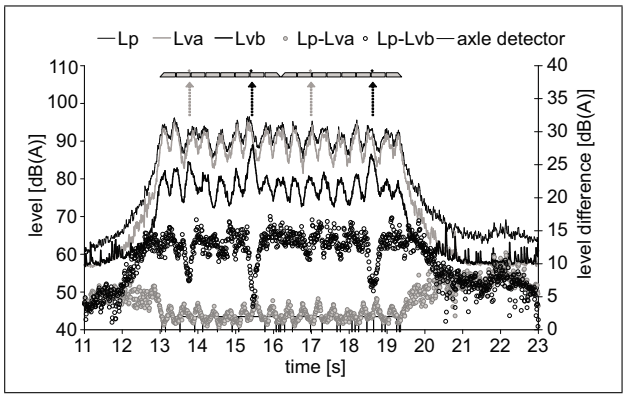


Figure 5. Temporal diagram of sound pressure L_p and sound velocity level L_{va} and L_{vb} of event F04, a pass-by of a double composition of a ICE 3 train type 403 at 228 km/h. The dotted arrows indicate the position of the pantographs with the turned on pantographs in black.



Figure 6. Picture of the roof section of an ICE 3 high speed train with a turned on pantograph. (Source: http://www.hochgeschwindigkeitszuege.com/galerie/de_ICE 3.html, photograph by André Werske).

passes the measurement cross section. As a consequence of the different directivity patterns the sound velocity level decreases more quickly than the sound pressure level when the bogie moves on and therefore the difference in level increases till the next bogie approaches. The velocity sensor *b* is oriented towards the roof section. As the sound emission from this area is generally smaller than from the wheel section the sound velocity level of sensor *b* are most of the time 10 to 15 dB(A) lower while the train passes the measurement section. At particular times of the pass-by the level difference between sound pressure and sound velocity *b* is though reduced significantly, for example in Figure 5 between 13 and 14 s, 15 and 16 s and between 18 and 19 s. This same pattern can also be found in the other measured pass-bys that are not separately depicted. Such a behaviour is a strong indication for the existence of prominent sound sources in the roof section. Based on the geometrical properties of the trains these sound sources in the roof section could be assigned to the first and last pantograph of composition one and to the last pantograph of composition two. In each case the last pantograph of the compositions was out which explains why they exhibit higher emission level. The difference in status of the first pantographs of composition one and two is not known. Therefore no explanation can be given why one appears as a prominent sound source and the other does not. Figure 6 shows a picture taken from above of an ICE 3-train. As can be seen the roof is generally highly streamlined with the exception of the pantograph, where turbulence and as a consequence aerodynamic sound sources are likely to emerge.

3.3. Source separation results

According to the procedure described in section 2 source separations were performed on the one hand for the entire train pass-bys and on the other hand for those parts of the pass-by in the vicinity of turned on pantographs. For this purpose a section of the measurement signals was analysed that yielded level differences between L_p and L_{vb} of less than 8 dB(A) around the local minimum, resulting in analysis times between 0.09 and 0.19 s and corresponding vehicle lengths between 5.3 and 11.7 m. Source positions were offered every 10 cm along an idealised vehicle surface for heights from -0.10 m to 5.70 m relative to rail level. The separation procedure was conducted for two sources with one source in the wheel section up to a height of 2 m and one in the upper part i.e. the roof section. Separations were performed once under the assumption of pure monopole sources and once for sources with a dipole directivity pattern. As the latter did not yield better accordance between measurements and calculations only the results for undirectedly radiating sources is shown.

Tables II and III show the results of the source separation. In Figure 7 the results are depicted graphically with the source position and sound power given for both analysed cases. Event *F11-2* is thereby highlighted as the separation procedure yielded a source position on the border of the given range of possible source positions. Such a result indicates that no local minima could be found during the optimization process of the source positions. Together with the high resulting error in Table III this can be taken as a strong hint for an overstressing of the optimization algorithm. Consequently results of event *F11-2* shall be neglected further on. A possible explanation for too high measurement errors within this event can be found in the analysis time that amounted to only 0.09 s and was significantly smaller than with all other analysed events. Generally it has to be beard in mind that short analysis times lead to an increase of measurement uncertainties, especially when looking at lower frequency bands. The advan-

tage of focussing on distinct parts of the pass-by in order to get smaller level differences between primary and secondary sources is therefore limited.

For all other events source positions were found within a narrow range. The centre of gravity of sound radiation for the wheel section was found at a height of 0.28 cm for the analysis of those parts of the pass-by with extended pantographs and at 0.36 cm for entire train pass-bys. This difference in height is clearly below the range of uncertainty of the localisation procedure. For the sources in the roof section a centre of gravity at 4.75 m and 3.37 m was derived for the two analysed situations. This can be taken as an indication that in the analysis of the entire train pass-bys not only the pantograph but also other aerodynamic sources at lower heights contribute to sound radiation. This interpretation is supported on the one hand by the resulting sound power for the sources in the roof section. While the average of the resulting sound power for the analysis of the sections with working pantographs amounts to 109.4 dB(A) the average for entire train pass-bys yields 112.3 dB(A). It can therefore be concluded that approximately 50% of the radiated sound in the roof section is stemming from the engaged pantographs while the remaining sound energy is contributed by other sources. Another indication for multiple sources in the roof section are the resulting errors in Tables II and III. They are comparably small within the pantograph section but much larger when looking at entire trains. This may suggest that the assumption of only two dominating sources was valid for the first but not for the second case. For entire train pass-bys the measured signals can not be reproduced with high accuracy when only two sound sources are provided in the model.

With an average sound power of 110.2 dB(A) the sound radiation from the wheel section is for working pantographs comparable to the contribution from the roof section. For entire train pass-bys rolling noise is though still the dominant source with an average of 124.2 dB(A) yielding about 12 dB(A) higher level than the roof section. It has to be pointed out though that aerodynamic sources can also occur within the wheel section. Figure 8 shows the dependency of the resulting sound power from the train speed. For pure rolling noise one would assume a linear dependency of $20 \ldots 30 \cdot \log(u)$ while aerodynamic sound sources feature with $50 \ldots 70 \cdot \log(u)$ significantly higher dependencies on the travelling speed. While the sources in the roof section show a behaviour typical for aerodynamic sources the dependency of the sources in the wheel section on $\log(u)$ is too great for rolling noise alone and therefore might be influenced by aerodynamic sources as well. It has to be mentioned though that the range of measured travelling speeds is rather small and therefore such conclusion have to be taken with caution.

Figure 9 shows the sound power spectra of the two sources within the range of working pantographs. While they exhibit comparable A-weighted level their spectral course deviates significantly. The spectrum of the source in the wheel section is typical for rolling noise with dominating frequencies around 1 kHz. In contrast the source in the roof section features far more energy that is radiated at lower frequencies.

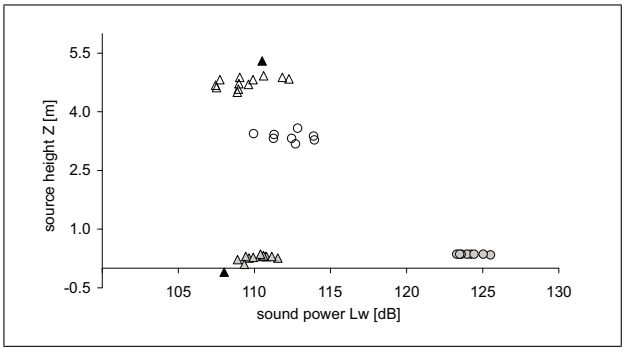


Figure 7. Source height vs. sound power for the analysis of entire train pass-bys (circles) and the sections with working pantographs (triangles), normalised to a train speed of 225 km/h. (The normalization has been done according to the dependency on the travelling speed depicted in Figure 8.) The highlighted event is *F11-2* where a source position on the border of the given range of possible source positions resulted.

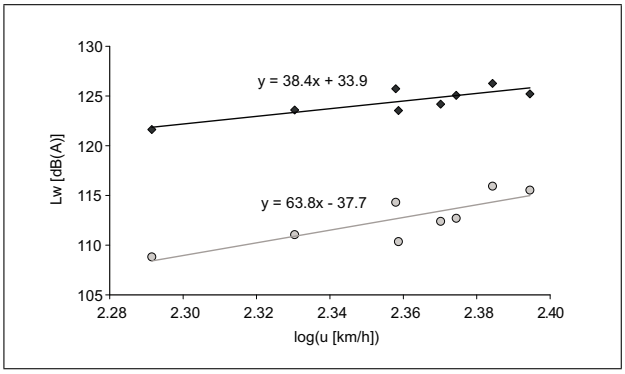


Figure 8. Resulting sound power of the sources in the wheel and roof section (black diamonds and grey circles respectively) in dependence of the travelling speed for a single composition of ICE 3 trains. Additionally depicted is the linear trend for both sources.

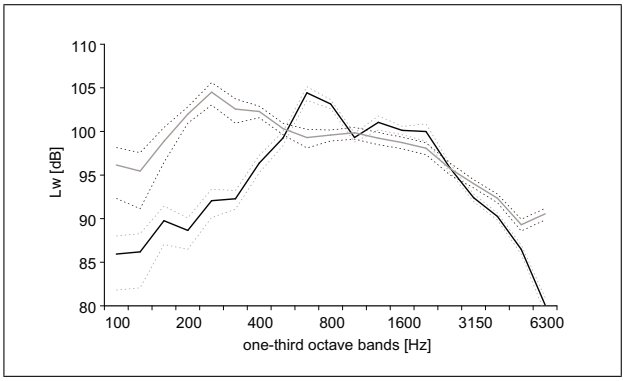


Figure 9. Sound power spectra of the sources in the wheel and roof section (black and gray curve respectively) of the parts with working pantographs, normalised to a train speed of 225 km/h. Additionally the 80% confidence intervals are given.

Table II. Results of the source separation based on entire train pass-bys, normalised to a single ICE 3-unit. u denotes the train speed. For the sources in the wheel and the roof section the position and the sound power of the identified centre of gravity of sound radiation on the vehicle are given. ΔL_{wA} indicates the sound power level difference between the two sources. In the last column the summed up deviation between the five measured A-weighted levels and their reproduction by calculation is given.

			Wheel section			Roof section				
Event	u [km/h]	log(u)	Y [m]	Z [m]	L_{wA}	Y [m]	Z [m]	L_{wA}	ΔL_{wA}	Error
F3	236.8	2.37	0.85	0.36	125.1	1.45	3.42	112.7	12.36	13.80
F4	228.4	2.36	0.85	0.36	123.5	1.45	3.44	110.4	13.18	15.99
F6	195.6	2.29	0.85	0.36	121.6	1.45	3.18	108.8	12.80	15.85
F7	248.0	2.39	0.85	0.36	125.2	1.37	3.58	115.5	9.67	9.67
F8	234.5	2.37	0.85	0.36	124.2	1.45	3.32	112.4	11.78	12.09
F9	228.0	2.36	0.85	0.34	125.7	1.45	3.28	114.3	11.42	13.19
F10	242.3	2.38	0.85	0.36	126.3	1.45	3.38	115.9	10.33	11.41
F11	214.0	2.33	0.85	0.36	123.6	1.45	3.32	111.0	12.55	14.40

Table III. Results of the source separation calculated for the part of the pass-by with working pantographs.

			Wheel section			Roof section				
Event	u [km/h]	log(u)	Y [m]	Z [m]	L_{wA}	Y [m]	Z [m]	L_{wA}	ΔL_{wA}	Error
F3-1	236.8	2.37	0.85	0.30	111.9	0.25	4.58	110.1	1.72	1.98
F4-1	228.4	2.36	0.85	0.26	110.0	0.25	4.72	109.3	0.64	2.02
F6-1	195.6	2.29	0.85	0.30	107.8	0.25	4.70	106.3	1.41	3.28
F7-1	248.0	2.39	0.85	0.30	112.6	0.25	4.84	114.5	-1.91	1.69
F8-1	234.5	2.37	0.85	0.30	110.3	0.25	4.88	110.0	0.33	2.13
F9-1	228.0	2.36	0.85	0.10	109.6	0.25	4.82	110.2	-0.59	3.76
F10-1	242.3	2.38	0.85	0.26	113.1	0.25	4.92	112.3	0.81	2.46
F11-1	214.0	2.33	0.85	0.30	110.1	0.25	4.88	110.7	-0.61	1.76
F3-2	236.8	2.37	0.85	0.28	111.0	0.25	4.82	108.9	2.10	2.11
F4-2	228.4	2.36	0.85	0.32	110.9	0.25	4.62	107.9	3.07	2.71
F6-2	195.6	2.29	0.85	0.36	107.4	0.25	4.50	105.6	1.75	1.63
F8-2	234.5	2.37	0.85	0.22	109.8	0.25	4.68	108.4	1.37	4.25
F11-2	214.0	2.33	0.85	*-0.10*	106.9	0.25	5.30	109.3	-2.41	20.23

4. Discussion of measurement results

The presented results are in good agreement with published data on ICE 3 measurements. Bechert *et al.* [20] also identified the dominating sound sources in the roof section at the pantographs. Barsikow [9] confirmed these results. Based on his array measurements two radiating parts could be separated close to the pantograph, the contact point of the traction wire and a second centre directly on the roof. Martens *et al.* [3] and Mellet et al. [21] found further sound sources in the upper section of the coaches, which were though all of minor importance relative to sources around the pantographs. Unfortunately a quantitative comparison with literature is not possible. On the one hand the mentioned publications mainly contain coloured maps that allow a localisation of sound sources but no numerical information on the attributed sound powers. On the other hand the operation conditions generally differed too much to be representative for the situation presented in this publication.

The resulting sound power of the sources in the roof section is within the measured velocity range significantly lower than the sound power in the wheel area. Even if the sound sources in the wheel area are to some extent aerodynamic sources it can be deduced that rolling noise still dominates the overall sound emission. The transition speed is therefore more likely around 300 km/h as predicted by Talotte [2]. Consequently it must be concluded that Dittrich [1] and Martens et al. [3] overestimated the importance of aerodynamic sources at least for the present measurement situation.

5. Comparison of the measurement method with array measurement technique

In many aspects the presented measurement method yields results that are comparable to those gathered with sophisticated arrays consisting of a great number of microphones. The accuracy of the derived sound power spectra is comparable, as well as the covered frequency range. And the signal-to-noise-ratio, i.e. the achievable difference in source level that still can be separated, seems to be at least as high as with array measurement technique.

The main advantage of the measurement concept in relation to array measurement technique lies in the measurement equipment and its simple application. The fact that only 3 to 4 measurement signals have to be calibrated, captured and processed in relation to up to 90 microphone signals as it is for example the case with the array of the German DB (see for example [22]) corresponds to a major simplification.

Additionally the use of directional probes allows a stronger local focussing. Out of focus contributions are highly suppressed and do not cause unwanted side lobes as it is often the case with array measurements (see for example [23]).

Negative aspects of the presented measurement concept in comparison to array measurements are that under practical conditions a separation of more than two sources can not be recommended as the measurement uncertainty increases significantly. Additionally the precision with which sound sources can be localised is generally smaller compared to array measurements.

These weaknesses lead to the conclusion that the measurement method can not be seen as a general replacement of the array measurement technique. For investigations where the focus lies on the localisation of the sources or where a higher number of partial sources have to be separated it is still necessary to use array measurement technique. This is for example the case for the collection of emission data for sophisticated calculation models as Harmonoise or sonRAIL.

In many situations the source positions are though already known or can be deduced from the physical properties of the vehicle. Additionally situations are very common where not more than two sound sources are relevant or where it is admissible to combine them into only two source areas, as it was done in this publication for the wheel and the roof section. In these cases the method is likely to represent an appropriate substitute for array measurements.

The range of application and the quality of its results is likely to be enhanced in the future. Efforts should be taken to reduce the measurement uncertainty, on the one hand by optimizing the sensor calibration and on the other hand by improving the accuracy of the propagation calculation. Mainly the ground effect model is currently not satisfactory and shall be replaced by a more sophisticated model. A third topic for improvements is the source description. The general assumption of incoherence is too restrictive and especially for rail noise not adequate in all aspects.

Acknowledgment

This work was supported by the Federal Office for the Environment of Switzerland (bafu) within the framework of sonRail, a project to develop an advanced calculation model for railway noise (see http://www.bafu.admin.ch/laerm/01146/06267/ for details). A special thanks goes to Deutsche Bahn AG, DB Systemtechnik, namely Mr. Gerbig, for the support during the measurement campaign.

References

[1] M. G. Dittrich, F. G. de Beer: The applicability of prEn ISO 3095 for European Legislation on Railway Noise. Final draft v3.2. TNO-report HAG-RPT-010014, February 28, 2001.

[2] C. Talotte: Aerodynamic noise a critical survey. Journal of Sound and Vibration **231** (2000) 549–562.

[3] A. Martens, J. Wedemann, N. Meunier, A. Lecere: High speed train noise - sound source localization at fast passing trains. Forum Acusticum, Sevilla, 2002.

[4] M. Dittrich: The IMAGINE model for railway noise prediction. Forum Acusticum, Budapest, 2005, 1237–1242.

[5] C. Talotte, P. van der Stap, M. Ringheim et al.: Railway source models for integration in the new European noise prediction method proposed in Harmonoise. Journal of Sound and Vibration **293** (2006) 975–985.

[6] D. Sehu, T. Thron: Entwicklung eines neuen Eisenbahnlärm-Berechnungsinstrumentes in der Schweiz- Projektmanagement, sonRAIL. ZEVrail **132** (2008) 261–264.

[7] A. Rohrbeck, T. Thron: sonRAIL - die Erweiterung des schweizerischen Lärmmodells für den Schienenverkehr. ZEVrail **132** (2008) 95–105. Tagungsband SFT Graz 2008.

[8] M. Hecht, T. Thron, Y. B. Othman: Einfluss von Rad- und Schienenrauheiten auf das Rollgeräusch - Messung und Berechnung. ZEVrail **132** (2008) 276–290.

[9] B. Barsikow: Experiences with various configurations of microphone arrays used to locate sound sources on railway trains operated by the DB AG. Journal of Sound and Vibration **193** (1996) 283–293.

[10] M. M. Boone, N. Kinneging, T. van den Dool: Two-dimensional noise source imaging with a T-shaped microphone cross array. Journal of the Acoustical Society of America **108** (2000) 2884–2890.

[11] K. G. Degen, A. Nordborg, A. Martens, J. Wedemann, L. Willenbrink, M. Bianchi: Spiral array measurements of high-speed train noise. Proceedings of the International Congress and Exhibition on Noise Control Engineering, Internoise, The Hague, 2001.

[12] A. Mast, T. C. van den Dool, J. D. van der Toorn, G. Watts, F. de Roo: HARMONOISE WP 1.1 - Source characterisation of moving vehicles with 'Acoustic Camera' antenna technique. Euronoise 2003, Naples, Itally, 2003.

[13] J. D. van der Toorn, H. Hendriks, T. C. van den Dool: Measuring TGV source strength with SYNTACAN. Journal of Sound and Vibration **193** (1996) 113–121.

[14] J. M. Wunderli: A measurement procedure for the sound emission of railway sources including source separation. Institution of Mechanical Engineers Vol. 219 Proceedings Part F: Journal of Rail and Rapid Transit **3** (2005).

[15] J. M. Wunderli: Quellenseparation bei fahrenden Zügen mit hilfe von Schalldruck- und Schallschnellemessungen. Shaker Verlag GmbH, 52018 Aachen, ISBN 978-3-8322-7009-4, 2008.

[16] International Standard ISO 9613-1: Acoustics - Attenuation of sound during propagation outdoors. Part 1: Calculation of the absorption of sound by the atmosphere. 1993.

[17] D. J. T. T. Kitagawa and: Comparison of wheel/rail noise radiation on Japanese railways using the TWINS model and microphone array measurements. Journal of Sound and Vibration **293** (2006) 496–509.

[18] F. J. Fahy: Sound intensity. Elsevier Science Publishers Ltd., ISBN 1-85166-319-3, 1989.

[19] H. E. de Bree: The microflown 2005. E-Book: www.microflown.com, 2005.

[20] D. W. Bechert, W. F. King III et al.: Schallquellenortung an schnellen Bahnfahrzeugen. DFVLR - Mitteilung 19-15, 1979.

[21] C. Mellet, F. Letourneaux, F. Poisson, C. Talotte: High speed train noise emission: Latest investigation of the aerodynamic/rolling noise contribution. Journal of Sound and Vibration **293** (2006) 535–546.

[22] C. Talotte, P.-E. Gautier, D. J. Thompson, C. Hanson: Identification, modelling and reduction potential of railway noise sources: a critical survey. Journal of Sound and Vibration **267** (2003) 447–468.

[23] J. J. Christensen, J. Harald: Beamforming. Brüel & Kjær, Technical Review Nr. 1, 2004.